AGU PUBLICATIONS

Geochemistry, Geophysics, Geosystems

RESEARCH ARTICLE
10.1002/2016GC006273

Key Points:
- We present a statistical method for identifying supply-limited and kinetic-limited chemical erosion
- Measured chemical erosion rates depend more strongly on mineral supply rate than weathering kinetics
- Our analysis implies that tectonics has a strong influence on Earth's chemical erosion thermostat

Supporting Information:
- Supporting Information S1

Correspondence to:
K. L. Ferrier,
ferrier@gatech.edu

Citation:
Ferrier, K. L., C. S. Riebe, and W. J. Hahm (2016), Testing for supply-limited and kinetic-limited chemical erosion in field measurements of regolith production and chemical depletion, *Geochem. Geophys. Geosyst.*, *17*, 2270–2285, doi:10.1002/2016GC006273.

Received 25 JAN 2016
Accepted 1 MAY 2016
Accepted article online 9 MAY 2016
Published online 24 JUN 2016

Testing for supply-limited and kinetic-limited chemical erosion in field measurements of regolith production and chemical depletion

Ken L. Ferrier[1], Clifford S. Riebe[2], and W. Jesse Hahm[3]

[1]School of Earth and Atmospheric Sciences, Georgia Institute of Technology, Atlanta, Georgia, USA, [2]Department of Geology and Geophysics, University of Wyoming, Laramie, Wyoming, USA, [3]Department of Earth and Planetary Science, University of California, Berkeley, Berkeley, California, USA

Abstract Chemical erosion contributes solutes to oceans, influencing atmospheric CO_2 and thus global climate via the greenhouse effect. Quantifying how chemical erosion rates vary with climate and tectonics is therefore vital to understanding feedbacks that have maintained Earth's environment within a habitable range over geologic time. If chemical erosion rates are strongly influenced by the availability of fresh minerals for dissolution, then there should be strong connections between climate, which is modulated by chemical erosion, and tectonic uplift, which supplies fresh minerals to Earth's surface. This condition, referred to as supply-limited chemical erosion, implies strong tectonic control of chemical erosion rates. It differs from kinetic-limited chemical erosion, in which dissolution kinetics and thus climatic factors are the dominant regulators of chemical erosion rates. Here we present a statistical method for determining whether chemical erosion of silicate-rich bedrock is supply limited or kinetic limited, as an approach for revealing the relative importance of tectonics and climate in Earth's silicate weathering thermostat. We applied this method to published data sets of mineral supply rates and regolith chemical depletion and were unable to reject the null hypothesis that chemical erosion is supply limited in 8 of 16 cases. In seven of the remaining eight cases, we found behavior that is closer to supply limited than kinetic limited, suggesting that tectonics may often dominate over climate in regulating chemical erosion rates. However, statistical power analysis shows that new measurements across a wider range of supply rates are needed to help quantify feedbacks between climate and tectonics in Earth's long-term climatic evolution.

1. Introduction

Chemical erosion plays a central role in sustaining life at Earth's surface. It helps create regolith from parent material, generating habitable substrates for life and liberating solutes from minerals, thus providing the foundation for ecosystem nutrient cycles [e.g., *Garrels and Mackenzie*, 1967; *Likens et al*., 1967; *Drever*, 1994; *Lucas*, 2001]. By influencing the chemistry of runoff, chemical erosion also influences the chemistry of Earth's oceans and atmosphere, with implications for global climate: changes in ocean alkalinity due to silicate dissolution modulate atmospheric CO_2 and thus regulate global temperature through the greenhouse effect [*Walker et al*., 1981; *Berner et al*., 1983]. But chemical erosion rates may depend on climate as well as regulate it, such that chemical erosion of silicates acts as a thermostat on global temperature [*Walker et al*., 1981; *Berner et al*., 1983]. Tectonic uplift may also play a role via its influence on production rates of regolith from parent material, which set the pace of fresh mineral supply for dissolution [*Raymo et al*., 1988; *Riebe et al*., 2004a, 2004b; *West et al*., 2005; *Colbourn et al*., 2015]. Hence, there may be strong links between chemical erosion, climate, and tectonics in Earth's long-term climatic evolution. Although these connections have been recognized for decades, the relative importance of climate and tectonics in the chemical erosion thermostat remains controversial.

Previous studies have cast chemical erosion of regolith in the context of two end-member conditions. In one end-member, chemical erosion rates increase proportionally with rates of fresh mineral supply from regolith production. Because chemical erosion rates are tightly coupled to mineral supply rates, this condition has been termed supply-limited chemical erosion [*Riebe et al*., 2004a, 2004b; *West et al*., 2005; *Gabet and Mudd*, 2009; *Hilley et al*., 2010; *Dixon et al*., 2012]. Across a suite of sites with differing mineral supply

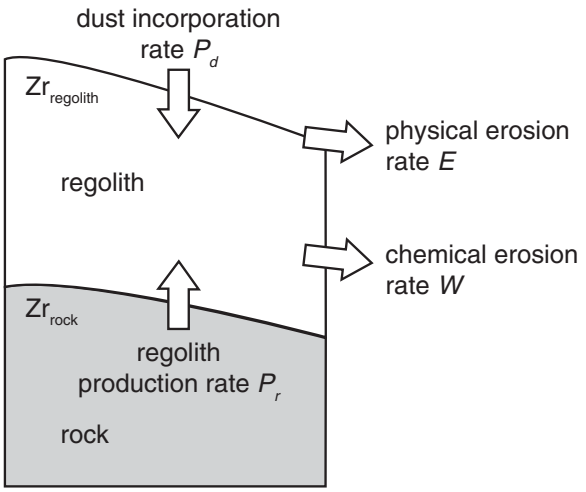

Figure 1. Schematic of a weathering profile on an eroding ridge. If the regolith is in steady state with constant composition and thickness, the mineral supply rate $S = P_r + P_d$ equals the total mass flux out of the regolith, which can be inferred from cosmogenic nuclide concentrations in soil or its parent rock. This flux can be partitioned into physical and chemical erosion rates (E and W) with measurements of rock-to-regolith enrichment of an immobile element (e.g., Zr), which reveals the chemical fraction of the total mass flux (*CDF*).

rates, regolith experiencing supply-limited chemical erosion would show the same degree of chemical depletion relative to parent material. Examples of this occur in the Amazon basin, where slowly eroding regolith is intensely weathered to a similar degree throughout the basin's lowlands [*Stallard and Edmond*, 1983], and across several sites in California's Sierra Nevada, where chemical erosion rates increase linearly with mineral supply rates [*Riebe et al*., 2001]. In a purely supply-limited condition, chemical erosion rates are tightly coupled to mineral supply rates, and thus are insensitive to climate, leading to weak feedbacks between weathering and climate [*West*, 2012; *Maher and Chamberlain*, 2014]. Nevertheless, in this condition, Earth's long-term climate could still be stabilized by silicate dissolution, to the extent that climate influences the overall degree of chemical depletion in regolith [*Riebe et al*., 2003, 2004b].

In the second end-member condition, the rate of chemical erosion—rather than the degree of chemical depletion—is invariant with mineral supply rates to the regolith. Thus, the degree of chemical depletion decreases with increasing mineral supply rates. Because chemical erosion rates in this condition are limited by the kinetics of mineral dissolution, this condition is often termed kinetic-limited chemical erosion [e.g., *West et al*., 2005; *Brantley and White*, 2009; *Brantley and Lebedeva*, 2011; *Brantley et al*., 2013]. Dissolution kinetics have been interpreted to be the dominant control on chemical erosion rates at the Shale Hills Critical Zone Observatory, Pennsylvania [*Jin et al*., 2010] and across water-limited granitic regions in the western United States and South Africa [*Rasmussen et al*., 2011]. Likewise, variations in stream solute fluxes across a compilation of catchments with fast erosion rates have been interpreted to reflect kinetic limitations on chemical erosion rates [*West et al*., 2005].

Here we focus on testing hypotheses about supply-limited and kinetic-limited chemical erosion with field measurements. We advocate that regolith-based measurements of chemical depletion and mineral supply rate are the most appropriate measurements to use in testing hypotheses about supply-limited and kinetic-limited chemical erosion. We show that chemical erosion rates tend to be more strongly influenced by supply rates than by dissolution kinetics across most sites where regolith-based measurements of chemical depletion and supply rates have been made. However, uncertainties are large, implying that future measurements across a wider range of supply rates will be helpful in testing hypotheses about tectonic and climatic controls on chemical erosion.

2. Framework for Supply-Limited and Kinetic-Limited Chemical Erosion

2.1. Conceptual Framework

We begin by describing a commonly used approach for measuring chemical erosion rates, mineral supply rates, and the degree of chemical depletion in eroding regolith. The data we will use to test hypotheses below are generated with this method, which is based on the geochemical mass balance of a steady-state column of regolith, in which the mass and bulk geochemistry of regolith remain constant over time. Figure 1 shows a schematic of a hillslope weathering profile with weathered regolith overlying unweathered bedrock and bordered on one side by a ridgetop.

In this study, we refer to the weathered material between the Earth's surface and the unweathered bedrock as regolith, consistent with usage in the geochemical literature [e.g., *Brantley and White*, 2009]. Because we focus on mass fluxes into and out of the regolith as a whole, we treat the regolith as a single layer. This is

similar to other conceptual models that treat the regolith as a single layer [e.g., *Riebe et al*., 2001; *Hilley et al*., 2010; *West*, 2012] and differs from studies that differentiate the regolith into a physically mobile layer and a physically immobile layer [e.g., *White et al*., 1998; *Anderson et al*., 2002; *Riebe et al*., 2003; *Yoo and Mudd*, 2008; *Dixon et al*., 2009a, 2009b]. While the consideration of multiple layers of regolith is not the focus of this study, the analysis presented here could be extended to do so.

The regolith mass balance is governed by the mass fluxes into and out of the regolith (Figure 1). Outgoing mass fluxes include the physical erosion rate, E [M L^{-2} T^{-1}], which is the rate at which solid particles are lost from the regolith, and the chemical erosion rate, W [M L^{-2} T^{-1}], which is the rate at which solutes are lost from the regolith. Incoming mass fluxes are collectively referred to as the mineral supply rate, S [M L^{-2} T^{-1}]. This includes the regolith production rate P_r, which is the rate at which the underlying rock is incorporated into the regolith, and the dust incorporation rate P_d, which is the rate at which minerals are added to the regolith through atmospheric deposition from above.

While dust deposition can dominate mineral supply to the regolith in settings with low regolith production rates and high dust fluxes [e.g., *Rex et al*., 1969; *Marchand*, 1970; *Brimhall et al*., 1988], as a global average over 90% of the minerals in regolith are derived from the underlying rock [*Ferrier et al*., 2011]. In many settings, dust deposition is a negligible component of the total mass flux into the regolith [i.e., $P_d \ll P_r$]. Because our goal is to test hypotheses about limits on chemical erosion rates, not to explore the role of dust deposition in modifying regolith chemistry, we followed previous studies and built our analysis on the approximation $S \approx P_r$ [e.g., *Riebe et al*., 2001, 2003, 2004a, 2004b; *Burke et al*., 2009, *Dixon et al*., 2009a, 2009b; *Larsen et al*., 2014a].

A few tools are commonly used to measure regolith mass fluxes over millennial timescales. Concentrations of cosmogenic nuclides in the mobile regolith or its underlying parent material reveal the regolith production rate [e.g., *Heimsath et al*., 1997; *Riebe et al*., 2001; *Foster et al*., 2015], as do vertical gradients in U-series disequilibria in unmixed regolith [e.g., *Dosseto et al*., 2012]. Given an estimate of the regolith production rate, the chemical erosion rate can be inferred from concentrations in regolith and parent material of so-called immobile elements—elements like Zr or Ti that remain in the regolith as more soluble elements are leached out [*Merrill*, 1897; *Marshall and Haseman*, 1942; *Stallard*, 1985; *Brimhall and Dietrich*, 1987; *Riebe et al*., 2001; *Ferrier et al*., 2012].

$$W = S\left(1 - \frac{Zr_{rock}}{Zr_{regolith}}\right) \tag{1}$$

Equation (1) specifies Zr as an example immobile element, and Zr_{rock} and $Zr_{regolith}$ are the concentrations of Zr in the rock and regolith, respectively.

The ratio of chemical erosion rates to mineral supply rates [i.e., W/S] is termed the chemical depletion fraction, or *CDF* [*Riebe et al*., 2001]. Rearranging equation (1) shows that it can be measured in steady-state regolith from the chemical differentiation of the regolith relative to its parent material [*Riebe et al*., 2001].

$$CDF = \frac{W}{S} = 1 - \frac{Zr_{rock}}{Zr_{regolith}} \tag{2}$$

This expression for *CDF* is similar to the formula used to calculate the geochemical mass transfer coefficient (now commonly denoted τ, after *Brimhall et al*. [1988]), but differs in that it expresses chemical losses of the regolith as a whole, rather than losses of individual elements. Values of *CDF* reflect the balance between mineral dissolution, which chemically depletes the regolith and increases *CDF*, and the supply of fresh minerals to the regolith, which chemically refreshes the regolith and decreases *CDF*.

2.2. Mathematical Framework

Supply-limited and kinetic-limited chemical erosion can be placed within a mathematical framework by writing the following power law relationship between chemical erosion rates and mineral supply rates.

$$W = aS^{b+1} \tag{3}$$

Equation (3) is a phenomenological relationship meant to help test hypotheses about supply-limited and kinetic-limited behaviors, rather than a relationship derived from a consideration of supply rates and

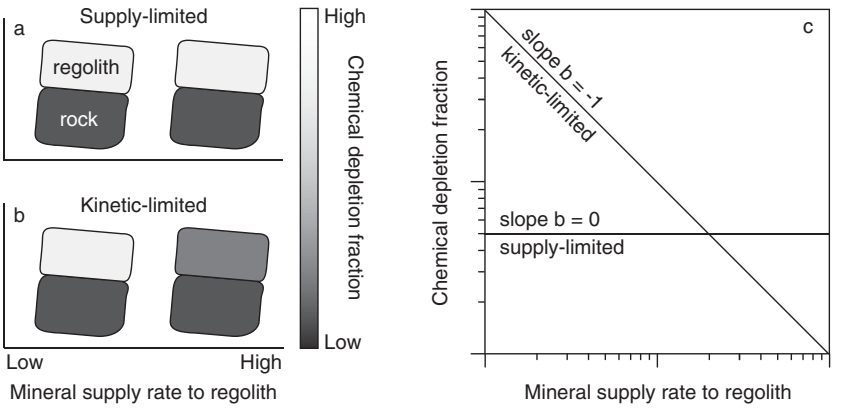

Figure 2. (a) Schematic of the condition necessary for supply-limited chemical erosion. This shows two hillslope weathering profiles: one with low mineral supply rates at left, and one with high mineral supply rates at right. Dark colors indicate little chemical depletion of regolith relative to the parent rock, and shading reflects grading from low (dark) to high (light) chemical depletion. In this supply-limited condition, the degree of regolith chemical depletion does not vary systematically with mineral supply rates. (b). In kinetic-limited chemical erosion, regolith chemical depletion decreases in inverse proportion to increasing mineral supply rates. (c) Graphical representation of supply-limited and kinetic-limited conditions. Note log scales on axes. The slope b is the exponent in equation (4).

dissolution kinetics [e.g., *Waldbauer and Chamberlain*, 2005; *Ferrier and Kirchner*, 2008; *Gabet and Mudd*, 2009; *Hilley et al*., 2010; *Maher and Chamberlain*, 2014]. We use equation (3) because it is the simplest possible power law relationship between chemical erosion rates and supply rates, and because it permits simple quantitative definitions of supply and kinetic limits. We stress that chemical erosion rates in nature need not follow a power law dependence on supply rates [e.g., *West et al*., 2005]. Likewise, the power law slope (b + 1) does not need to be constant across all supply rates; models of dissolution kinetics generally predict changes in the slope as chemical erosion changes from supply limited at low supply rates to kinetic limited at high supply rates. Equation (3) is useful because it provides quantitative definitions for supply-limited and kinetic-limited behaviors, and is therefore useful for testing hypotheses about those limits, which is the main goal of this study.

Because CDF is the fraction of the total erosion rate caused by chemical erosion (equation (2)), equation (3) can be expressed in equivalent form in equivalent form in equation (4).

$$CDF = W/S = aS^{b} \tag{4}$$

For this study, the most important quantity in equations (3) and (4) is b, the power law slope of the relationship between *CDF* and *S*. In supply-limited chemical erosion, b = 0 because chemical erosion rates are proportional to supply rates and *CDF* is invariant with supply rates (Figure 2). In kinetic-limited chemical erosion, b = −1 because chemical erosion rates are invariant with supply rates and *CDF* is inversely proportional to supply rate (Figure 2).

2.3. Using CDF and Mineral Supply Rate in a Framework for Interpreting Chemical Erosion Rates

Because b is a power law slope in equation (4), it can be estimated via curve fitting using independent measurements of *CDF* and *S*. Thus, we can use the exponent b to test hypotheses about supply-limited and kinetic-limited chemical erosion. If b is equal to 0 within error, then it implies that the data are consistent with supply-limited chemical erosion, characteristic of tectonic control on chemical erosion rates. If b is instead equal to −1 within error, then it implies that the data are consistent with kinetic-limited chemical erosion, characteristic of climatic control on chemical erosion rates. Alternatively, values of b between 0 and −1 imply intermediate conditions; chemical erosion rates still increase with supply rates, but not in direct proportion, implying that there is a mix of kinetic (e.g., climatic) and supply-related (e.g., tectonic) controls on silicate dissolution.

In principle, the same is true for the power law exponent b + 1 in equation (3). For example, if b + 1 = 1, then it implies that the data are consistent with supply-limited chemical erosion. However, in practice, because *W* is calculated from *S* in regolith-based estimates of chemical erosion (e.g., using equation (1)), regressions of *W* against *S* are prone to biases due to spurious correlation. That is, the correlation coefficient

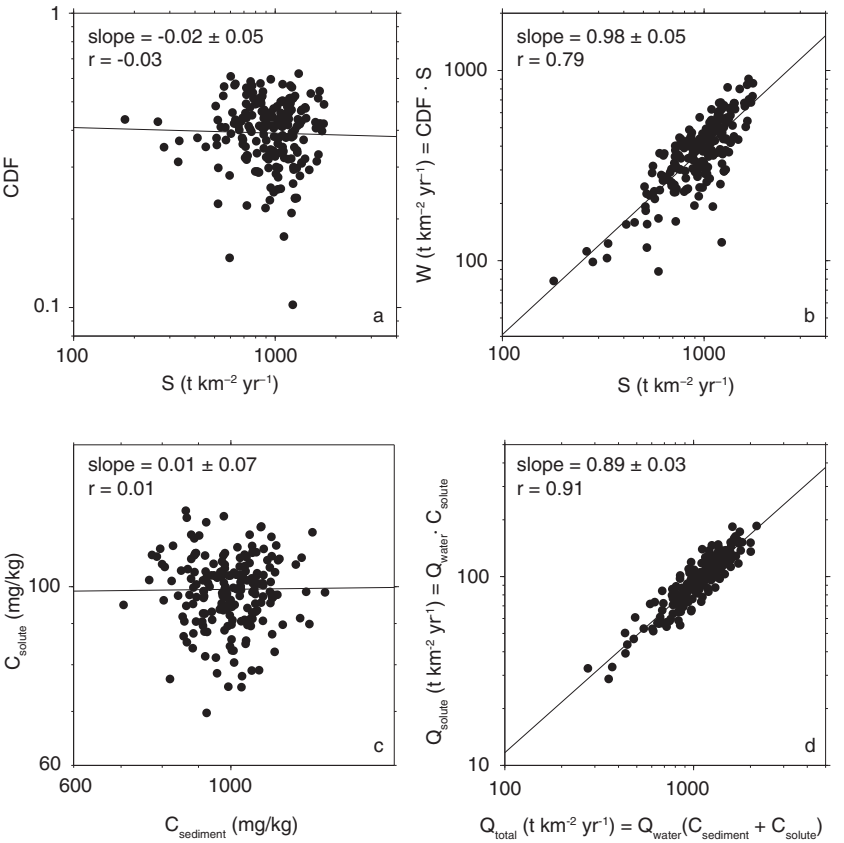

Figure 3. Spurious correlation in regolith-based and fluvial-based measurements of chemical erosion rates. (a) Synthetic data set of 200 random, normally distributed, and uncorrelated regolith-based *CDF* and *S* values. The low correlation coefficient reflects the lack of a dependence of *CDF* on *S* in this hypothetical example. (b) A regression of *W* (*CDF*·*S*; equation (1)) against *S* for the same data set has a high r. This spuriously high r value arises from the presence of *S* on both axes. (c) Synthetic data set of 200 random, normally distributed, and uncorrelated concentrations of suspended sediment ($C_{sediment}$) and solutes (C_{solute}) in stream water. The mean and standard deviation of $C_{sediment}$ are 1000 and 100 mg/kg, respectively, while the mean and standard deviation of C_{solute} are 100 and 10 mg/kg, respectively. (d) A power law regression of the solute flux $Q_{solute} = (Q_{water} \cdot C_{solute})$ against the total mass flux $Q_{total} = (Q_{water}\,[C_{sediment} + C_{solute}])$ has a spuriously high r, which is a result of the presence of Q_{water} and C_{solute} on both axes. Here we assume that both the bed load and suspended sediment load are represented by $C_{sediment}$. We generated values of Q_{water} using a random sample from a normal distribution with mean $= 10^6$ t km^{-2} yr^{-1} and standard deviation $= 3{\cdot}10^5$ t km^{-2} yr^{-1}.

r, which expresses the goodness of fit in a y versus x regression, is likely to differ from zero (and thus indicate some correlation exists) when x and y share a common variable, even if the underlying independent variables are uncorrelated with one another [*Pearson*, 1897; *Reed*, 1921; *Chayes*, 1949; *Bensen*, 1965; *Kenney*, 1982, *Galat*, 1990, *Brett*, 2004]. Thus, when r is calculated for a regression between *W* and *S*, it will overestimate the correlation between the rates of chemical erosion and mineral supply when equation (1) is used to calculate the chemical erosion rate (i.e., as a fraction of the mineral supply rate). In contrast, regolith-based measurements of *CDF* (using Zr concentrations) and *S* (using cosmogenic nuclides) are independent of one another. Thus, regressions of *CDF* against *S* are not generally prone to spurious correlation in regolith-based studies of chemical erosion.

The potentially confounding effects of spurious correlation are illustrated in a hypothetical example shown in Figure 3. *CDF* is plotted against *S* for an uncorrelated set of synthetic data. Each *CDF* value was randomly selected from a normal distribution with a mean of 0.4 and standard deviation of 0.1, while each *S* value was randomly selected from a normal distribution with a mean of 1000 t km^{-2} yr^{-1} and standard deviation of 300 t km^{-2} yr^{-1}. These synthetic *CDF* and *S* values span a range that is typical of observations from field studies (e.g., supporting information Table S1). The intrinsic lack of correlation between chemical depletion and mineral supply rates in the synthetic data set is reflected in the low r (0.03) and a power law regression slope that is indistinguishable within error from 0 (Figure 3a). In contrast, when we plot *W* calculated as the product *S*·*CDF* against *S*, we observe a statistically significant r of 0.79 and a best fit power law slope of

0.98 ± 0.05 (Figure 3b). The high r in Figure 3b is the signature of the spurious correlation. It is a mathematical consequence of the existence of S on both axes, rather than a mechanistic reflection of the strength of the dependence of W on S.

Spurious correlation affects fluvial-based estimates of chemical and physical erosion rates [e.g., *Galat*, 1990] in much the same way it affects regolith-based estimates from equations (1) to (4). However, in fluvial-based estimates, physical erosion rates E are generally calculated as $E = Q_{sediment} = Q_{water} \cdot C_{suspended} + Q_{bedload}$ (or a similar formula), where Q_{water} [M L^{-2} T^{-1}] is the stream water discharge per unit drainage area, $C_{sediment}$ [M M^{-1}] is the suspended sediment concentration in stream water, and $Q_{bedload}$ [M L^{-2} T^{-1}] is the bedload sediment flux. Similarly, chemical erosion rates are calculated as $W = Q_{solute} = Q_{water} \cdot C_{solute}$, where C_{solute} [M M^{-1}] is the solute concentration in stream water. In steady state, mineral supply rates to the regolith equal the sum of sediment and solute fluxes ($S = E + W$) and $CDF = W/S$. Thus, in fluvial-based studies of erosion, W and S are based on the same measurements of Q_{water} and C_{solute}, while CDF is determined from S. As a result, regressions of both W against S and CDF against S will have correlation coefficients that are biased by spurious correlation. Thus, even when there is no underlying relationship between $C_{sediment}$ and C_{solute} (Figure 3c), a correlation between solute loading rates ($W = Q_{solute}$) and total loading rates ($S = Q_{sediment} + Q_{solute}$) will be evident (Figure 3d). A power law regression between the synthetic W and S values in Figure 3d yields a best fit slope of 0.89 ± 0.03 and an r of 0.89. The high r in Figure 3d reflects a spurious correlation that results from the presence of Q_{water} and C_{solute} on both axes.

We stress that Figures 3a–3d are drawn from hypothetical distributions, and that real-world measurements of these variables can deviate from the trends in Figure 3. For instance, measurements of fluvial solute and sediment fluxes show that plots of W versus $W + E$ deviate from a 1:1 line [e.g., *West et al.*, 2005], implying that fluvial flux data do not conform to supply-limited behavior at high supply rates. Because such plots share a variable on the x and y axes, however, r values drawn from such plots must be subject to spurious correlation to some degree.

This is not to say that fluvial solute fluxes are inherently subject to spurious correlation; it depends only on what they are regressed against. For instance, spurious correlation can be avoided if solute concentrations (rather than solute fluxes) are plotted against discharge [e.g., *Godsey et al.*, 2009; *Torres et al.*, 2015]. Fluvial solute flux data can avoid spurious correlation if plotted against basin-averaged supply rates inferred from cosmogenic nuclides in stream sediment, because these data types are drawn from independent measurements. Alternatively, r values between terms that share a common index (like discharge) can be compared against the expected purely spurious correlation that arises when the underlying variables are independent [*Pearson*, 1897]. We do not consider the combination of those two data types further, because such regressions can be complicated by factors unrelated to spurious correlation, such as the different timescales of each measurement (typically annual to decadal for fluvial fluxes and millennial for cosmogenically inferred supply rates) [*Kirchner et al.*, 2001], or perturbations in cosmogenic nuclide concentrations by landsliding [e.g., *Brown et al.*, 1995; *Niemi et al.*, 2005; *Yanites et al.*, 2009; *West et al.*, 2014], spatial variations in the grain size of sediment delivered to the channel [*Riebe et al.*, 2015; *Lukens et al.*, 2016], and spatially variable particle paths downslope within the regolith [*Foster et al.*, 2015; *Anderson*, 2015].

The two examples in Figure 3 show that regressions of W against S are subject to spurious correlation, both for regolith-based and fluvial-based measurements of catchment inputs and outputs. This arises because estimates of W and S are based on the same data. In contrast, regolith-based measurements of CDF and S in equation (4) are independent of one another. Thus, regressions of CDF against S are not subject to spurious correlation, provided that they are determined from independent measurements in regolith. For this reason, we use regolith-based measurements of CDF and S for testing hypotheses about chemical erosion in this study.

2.4. Definitions of Supply-Limited and Kinetic-Limited Chemical Erosion as End-Member Conditions

In this study, we use the terms supply-limited and kinetic-limited chemical erosion to refer strictly to end-member behaviors defined by $b = 0$ and $b = -1$, respectively, in equation (4). These definitions have two important implications. The first is that chemical erosion in any system characterized by $-1 < b < 0$ is neither supply limited nor kinetic limited but instead is influenced both by rates of mineral supply and by mineral dissolution kinetics. This intermediate regime corresponds to a transitional regime described in other studies [e.g., *Lebedeva et al.*, 2010; *Rasmussen et al.*, 2011]. Moreover, the definition of kinetic-limited

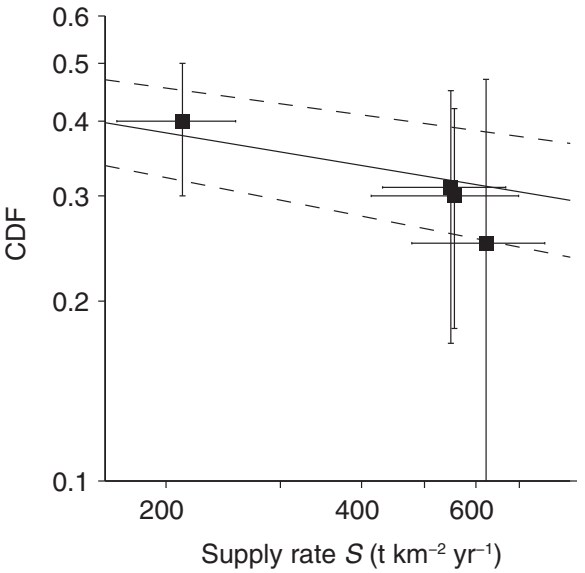

Figure 4. Chemical depletion fraction (*CDF*) versus mineral supply rate at Jalisco Highlands, Mexico (mean ± 2 SE) [*Riebe et al*., 2004b]. The solid line shows the regression of log(CDF) against log(supply rate), and has a power law slope of b = −0.37 ± 0.07 (mean ± 95% confidence interval), which can be used to test for supply-limited and kinetic-limited chemical erosion at this site (see Figure 2). Dashed lines show 95% confidence intervals for regression line.

behavior as b = −1 is distinct from the implication that any behavior that is not supply limited is kinetic limited [e.g., *Brantley and White*, 2009; *Norton and von Blanckenburg*, 2010; *Jin et al*., 2010; *Lebedeva et al*., 2010; *Ferrier et al*., 2012]. This definition of "kinetic limited" is useful because it shares an important mathematical characteristic with the definition of "supply limited." That is, the definition of "kinetic limited" as b = −1 represents a limiting behavior, just as "supply limited" represents the limiting behavior of b = 0. In this terminology, values of b that lie between those limits thus imply that chemical erosion rates are *influenced* by both mineral supply and dissolution kinetics, rather than *limited* by one or the other.

The second implication of these definitions is that the regolith does not need to be weathered to completion (i.e., *CDF* does not need to equal 1) for chemical erosion to be supply limited. Instead, the regolith only needs to be chemically depleted to the same degree across a range of supply rates for supply-limited conditions to hold. This has been observed in some field studies. For instance, at Fall River and Fort Sage [*Riebe et al*., 2001; Figure 5], *CDF* does not vary systematically with supply rates even though these sites have *CDF* values (<0.2) that are consistent with incomplete dissolution of commonly weatherable minerals such as feldspar and biotite. Indeed, except in the case of carbonate bedrock, it is impossible for *CDF* = 1, and even then it would be impossible to measure *CDF*, because in this limit all minerals would be completely dissolved and the regolith itself would not exist. Thus, in all applications of the approach, *CDF* will be less than 1. This is consistent with studies that have noted that some fraction of the parent rock should be effectively insoluble over the regolith residence time in many mountainous environments, which should prevent *CDF* values from growing higher than some effective maximum *CDF* that is less than 1 [e.g., *West et al*., 2005; *Hilley et al*., 2010]. The existence of an effective maximum *CDF* does not affect the best fit b value, which depends only on the relationship between log(*CDF*) and log(*S*), not their magnitudes. Such an upper limit on *CDF* therefore does not hinder hypothesis testing about supply-limited and kinetic-limited chemical erosion.

3. Methods

Our analysis hinges on being able to distinguish the regression slope of a log(*CDF*) versus log(*S*) relationship from the limiting conditions of b = 0 and b = −1. We do so using classical statistical hypothesis testing. Thus, our analysis relies critically on quantifying the uncertainties in the regression parameters, which in this case reflect both the scatter in the log(*CDF*) versus log(*S*) relationship and any measurement uncertainties in log(*CDF*) and log(*S*). These sources of uncertainty obscure our ability to differentiate between supply-limited and kinetic-limited chemical erosion in natural settings.

To understand how, consider the null hypothesis that chemical erosion is supply limited. This is equivalent to stating that the true slope, b_0, is zero. To evaluate this hypothesis for each data set, we computed Student's *t*, where $t = (b - b_0)/s_b$, and s_b is the standard error of the mean slope (Table 1). Next, we compared the t to $t_{\alpha,\nu}$, where the degrees of freedom, ν, is equal to the number of measurements minus 2, and the user-defined risk, α, that the null hypothesis will be mistakenly rejected if it is actually true, is 0.05 (i.e., 5% false positive rate) in a two-tailed t-test. If $t > t_{\alpha,\nu}$, then the null hypothesis is rejected. Otherwise, it is not

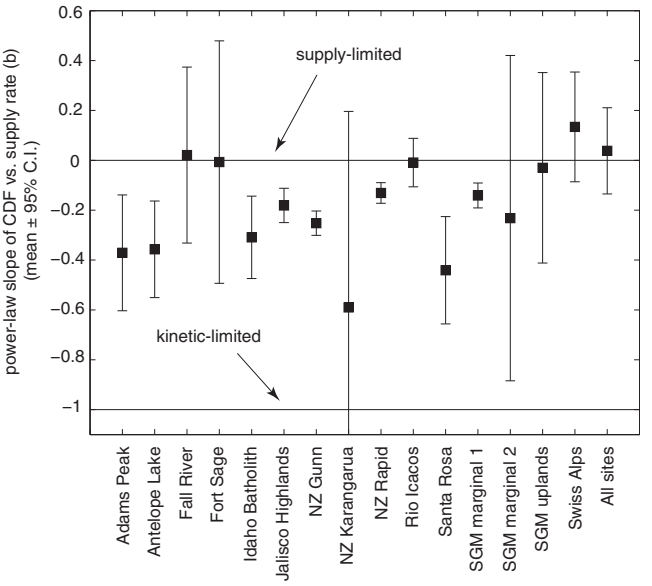

Figure 5. Mean ± 95% confidence intervals of power law slope b for regressions of *CDF* versus *S* from published studies [*Riebe et al*., 2001, 2003, 2004a, 2004b; *Norton and von Blanckenburg*, 2010; *Dixon et al*., 2012; *Ferrier et al*., 2012; *Larsen et al*., 2014a]. A slope of −1 indicates kinetic-limited chemical erosion, and a slope of 0 indicates supply-limited chemical erosion (Figure 2). Many slopes are not significantly different from 0, and those that are different plot closer to 0 than −1. To the extent that values of b close to 0 reflect a dominance of supply over kinetics in driving chemical erosion, this suggests that chemical erosion is influenced more strongly by mineral supply rates than by dissolution kinetics.

rejected. We used a similar process to test the null hypothesis that chemical erosion is kinetic limited (i.e., $b_0 = -1$).

We applied the test in Figure 2 to data sets from 15 studies that have published *CDF*s, mineral supply rates, and estimates of uncertainties for at least four independent catchments or soil profiles [*Riebe et al*., 2001, 2003, 2004a, 2004b; *Norton and von Blanckenburg*, 2010; *Dixon et al*., 2012; *Ferrier et al*., 2012; *Larsen et al*., 2014a]. We also performed a collective test of supply-limited and kinetic-limited chemical erosion on all the data combined in a single group. We computed best fit values of a and b in equation (4) using Gaussian process regression [e.g., *Rasmussen and Williams*, 2006; *Hay et al*., 2015] on values of log(CDF) and log(S). Because this method accounts for inter-sample scatter and for measurement uncertainties in *x* and *y* directions and is robust against outliers in small data sets, it is well suited for quantifying power law slopes for the *CDF* and supply rate data compiled here (supporting information Table S1). Each study was conducted in a region of uniform lithology of granite, granodiorite, or schist. By design, we used measurements from studies that have little site-to-site variation in lithology, to minimize the potentially confounding effects of differences in mineralogy on chemical erosion rates. Likewise, within many of these data sets, sites were close enough to each other that they share a similar climate, thus minimizing potentially confounding effects of differences in climatic factors that might influence chemical erosion rates. Climate varies substantially among the studies but varies little among sites at most of the studies. Mean annual precipitation (MAP) at the study sites ranges from 25 to 1152 cm, and mean annual temperature (MAT) ranges from −5.5 to 23°C (Table 1).

4. Data and Results

4.1. Best Fit Values for Regression Parameters

Best fit values of b computed with Gaussian process regression range from -0.590 ± 0.247 to 0.134 ± 0.101 (mean ± SE) (Table 1). A comparison of best fit values for regression parameters computed with other regression methods is provided in the supporting information. Figure 4 shows an example of regression results for one of the study sites. Analogous figures for each of the other data sets considered in this study are provided in the supporting information.

4.2. Most Power Law Regression Slopes Are Closer to b = 0 (Supply Limited) Than to b = −1 (Kinetic Limited)

Figure 5 shows best fit values of b, plus or minus their uncertainties, for each of the study sites under consideration, as well as for a regression through all the data from all studies (labeled "All sites" in Figure 5). Across these data sets, values of b range from -0.59 ± 0.79 to 0.13 ± 0.22 (mean ± 95% confidence interval), with an inverse variance-weighted mean of -0.17 ± 0.05 (mean ± 95% confidence interval). The best fit value of b in a regression to all data from all these studies is 0.04 ± 0.17, consistent with supply-limited chemical erosion.

Table 1. Study Site Characteristics and Best Fit Regression Parameters in $CDF = aS^b$ (Equation (4))

Site	Lat. (°N)	Long. (°E)	MAT[a] (°C)	MAP[a] (cm)	n[b]	$t_{critical}$[c]	log(a) (Mean ± SE)	b (Mean ± SE)	Std. of log(*S*)	RMSE[d]	Reject $b_0 = 0$?[e]	Reject $b_0 = -1$?[e]	Ref.[f]
Adams Peak	39.88	−120.07	3.3–5.5	51–63	5	3.182	4.67E-4 ± 6.99E-2	−0.371 ± 0.073	0.10	0.38	Yes	Yes	1
Antelope Lake	40.17	−120.63	7.6–8.2	79–85	4	4.303	2.36E-5 ± 1.18E-2	−0.357 ± 0.045	0.07	0.14	Yes	Yes	1
Fall River	39.65	−120.32	10.7–13.5	140–152	4	4.303	−0.754 ± 0.176	0.021 ± 0.082	0.47	0.09	No	Yes	1
Fort Sage	40.17	−120.07	12.0–12.5	25–28	4	4.303	−0.782 ± 0.275	−0.007 ± 0.113	0.48	0.30	No	Yes	1
Idaho Batholith	45.12	−115.60	4.8–10.9	65	16	2.145	−0.229 ± 0.157	−0.309 ± 0.077	0.19	0.29	Yes	Yes	7
Jalisco Highlands	20.35	−105.30	23	180	4	4.303	9.15E-9 ± 1.00E-4	−0.181 ± 0.016	0.22	0.07	Yes	Yes	4
N.Z. Gunn	−43.40	170.40	No data	No data	7	2.571	1.24E-4 ± 1.31E-2	−0.252 ± 0.019	0.14	0.17	Yes	Yes	8
N.Z. Karangarua	−43.65	169.85	No data	No data	5	3.182	1.09 ± 0.689	−0.590 ± 0.247	0.22	0.94	No	No	8
N.Z. Rapid	−43.03	171.02	5.5	1152	5	3.182	1.68E-8 ± 1.00E-4	−0.131 ± 0.013	0.29	0.13	Yes	Yes	8
Rio Icacos	18.30	−67.80	22	420	6	2.776	−0.190 ± 0.081	−0.009 ± 0.035	0.02	0.03	No	Yes	2
Santa Rosa	41.50	−117.63	−0.4–3.6	54–83	4	4.303	−3.16E-5 ± 4.66E-2	−0.441 ± 0.050	0.06	0.25	Yes	Yes	3
SGM marginal 1	34.35	−118.03	13.3	79	6	2.776	−1.65E-5 ± 4.20E-3	−0.141 ± 0.018	0.08	0.11	Yes	Yes	6
SGM marginal 2	34.37	−118.00	12.2	77	6	2.776	0.033 ± 0.575	−0.232 ± 0.235	0.12	0.44	No	Yes	6
SGM uplands	34.35	−118.00	12.1	83	5	3.182	−0.357 ± 0.237	−0.030 ± 0.120	0.31	0.11	No	Yes	6
Swiss Alps	46.50	8.20	−5.5 to 0.3	114	14	2.179	−0.729 ± 0.221	0.134 ± 0.101	0.19	0.14	No	Yes	5
All sites					95	1.986	−0.719 ± 0.209	0.038 ± 0.087	0.43	0.34	No	Yes	

[a]MAT = mean annual temperature. MAP = mean annual precipitation. For MAT and MAP, single values indicate that only one value was reported in the original study, while ranges indicate the range of values between sites in that study.

[b]n = number of colocated measurements of *CDF* and supply rate *S*. See supporting information Table S1 for all *CDF* and *S* measurements.

[c]$t_{critical}$ = critical value of Student's *t* distribution at a significance level $\alpha = 0.05$ and degrees of freedom $\nu = n - 2$ in a two-tailed t-test [e.g., *Zar*, 1999]. Ninety-five percent confidence intervals for regression parameters are calculated as the parameter's standard error multiplied by $t_{critical}$. For example, at Adams Peak, the mean and 95% confidence interval for the slope b is $-0.371 \pm (3.182 \cdot 0.073) = -0.371 \pm 0.232$.

[d]RMSE = root-mean-square error, which is the standard deviation of log(*CDF*) values from the regression line log(*CDF*) = a + b log(*S*).

[e]Null hypotheses $b_0 = 0$ (supply-limited chemical erosion) and $b_0 = -1$ (kinetic-limited chemical erosion) were tested with a statistical significance $\alpha = 0.05$.

[f]Reference codes: 1 = *Riebe et al.* [2001]; 2 = *Riebe et al.* [2003]; 3 = *Riebe et al.* [2004a]; 4 = *Riebe et al.* [2004b]; 5 = *Norton and von Blanckenburg* [2010]; 6 = *Dixon et al.* [2012]; 7 = *Ferrier et al.* [2012]; 8 = *Larsen et al.* [2014a].

5. Discussion

Next, we describe our statistical tests of supply-limited versus kinetic-limited chemical erosion. We also discuss the tendency toward 0, within error, for many of the power law slopes in Figure 5. We suggest that this tendency indicates that the tectonic effects that influence mineral supply rates may often be more important in regulating chemical erosion rates than climate across the study sites examined here.

5.1. Implications for Feedbacks Between Topography, Tectonics, and Climate

Figure 5 shows that 7 of the 15 data sets have values of b that are indistinguishable from zero within 95% confidence intervals, which implies that a null hypothesis of supply-limited chemical erosion cannot be rejected, given the chosen significance threshold of $\alpha = 0.05$ and the number of measurements in the data sets. Only one of the data sets has a value of b that is indistinguishable from −1, but it is also indistinguishable from 0, indicating that the uncertainties are too large to draw any conclusions about supply-limited and kinetic-limited behavior. The remaining eight data sets have values of b that do not overlap with either 0 or −1 within their 95% confidence bounds, implying that chemical erosion rates are neither supply limited nor kinetic limited, but instead are influenced by both supply rates and dissolution kinetics. The estimated values of b for these remaining data sets lie between 0 and −0.5.

This analysis has implications for understanding the feedbacks between topography, tectonics, and climate that influence the evolution of Earth's land surface. The main message of Figure 5 is that best fit values of b in these studies tend to be closer to 0 than to −1. That is, even though the average behavior of chemical erosion rates across these sites is not supply limited (i.e., the mean b is not 0), it is not far from supply limited (i.e., the mean $b = -0.17 \pm 0.05$). To the extent that values of b close to 0 reflect a dominance of supply over kinetics in driving chemical erosion, this suggests that chemical erosion rates at these sites are more sensitive to mineral supply rates than mineral dissolution kinetics.

If these results are broadly applicable to other landscapes and other lithologies, they imply that the feedback between tectonic uplift, silicate dissolution, and climate is strong—though not as strong as it would be if chemical erosion rates were purely supply limited. This in turn suggests that the silicate weathering thermostat should be strongly dependent on mineral supply rates to the regolith, but also somewhat dependent on factors that influence mineral dissolution (e.g., water fluxes through the regolith, and

ambient temperature). A weak dependence of silicate dissolution on climate poses challenges for explaining how Earth's climate has stayed in a habitable range over time despite variations in geologic forcing (e.g., due to changes in insolation or degassing during arc volcanism) [*Lee et al*., 2015]. In a supply-dominated world, one way that climate could exert sufficient control on silicate dissolution to induce a strong weathering-climate feedback is by influencing the overall degree of chemical depletion on hillslopes. For example, if increases in global temperature increase *CDF*s, thereby changing the intercept – but not the slope – of the relationship between CDF and supply rate, they would increase loading of alkalinity to the oceans, which would consume atmospheric CO_2 and reduce global temperatures. Even if the influence of climate on *CDF* is minimal, our finding of a tendency toward supply-limited chemical erosion does not preclude a strong silicate dissolution thermostat: our analysis was focused solely on regolith in mountainous settings and thus cannot reveal anything about potentially stronger connections between climate and chemical erosion in low-lying areas, which encompass the majority of Earth's land surface [e.g., *Lupker et al*., 2012; *Willenbring et al*., 2013; *Kirchner and Ferrier*, 2013; *Larsen et al*., 2014b].

5.2. Statistical Power Analysis

The statistical test described in section 2 is designed to test hypotheses about limits on chemical erosion. In applications of the test to a data set of *CDF* and *S* estimates, it is worth asking whether the test is reliable at detecting a given difference between the measured slope b and the null hypothesis slope b_0, given a threshold significance level α and the measured uncertainty in the slope, s_b. How confident can we be that the test will not incorrectly suggest that chemical erosion is supply limited when it actually is not? In other words, how sure can we be that our test will avoid false negatives when testing the null hypothesis that chemical erosion is supply limited? Similarly, we can ask, what is the chance of false negatives in our test of the null hypothesis that chemical erosion is kinetic limited?

The answer to these questions depends on four quantities: (1) the deviation δ of the measured slope from either 0 (for a supply limitation) or -1 (for a kinetic limitation), where $\delta = |b - b_0|$; (2) the uncertainty in the measured slope, s_b; (3) the user-defined statistical significance level, α; and (4) the degrees of freedom $\nu = n - 2$, where n is the number of measurements. These quantities define $t_{\beta,\nu}$, in which β is the likelihood that the test will incorrectly conclude that chemical erosion is supply limited when it is not, also known as the false negative rate.

$$t_{\beta,\nu} = \delta / s_b - t_{\alpha,\nu} \tag{5}$$

The complement of the false negative rate is $1 - \beta$, which is the likelihood that the test will avoid false negatives. It is a measure of the reliability of the test, known as the statistical power. It is the quantity of interest here. Values of β can be calculated from values of $t_{\beta,\nu}$ in equation (5) and one-tailed values of Student's *t* statistic.

As described in section 3, we used Gaussian process regression to determine best fit values of b and s_b. Because Gaussian process regression is a Bayesian iterative procedure, there are no analytic expressions for b and s_b as a function of the input *CDF* and *S* data, which means that there is no analytic expression for the method's statistical power as a function of the input data. We therefore determined the method's statistical power empirically with a Monte Carlo simulation.

The Monte Carlo simulation is rooted in synthetic sets of *CDF* and *S* data, which we generated at prescribed pairs of n and std(log(*S*)) values. We chose to prescribe n because it is one of the few quantities under the user's control when designing a field study, and because we wanted to explore how the user's choice of n influences the method's statistical power.

We chose to prescribe std(log(*S*)) because it is a measure of the spread in log(*S*), which, as the quantity on the *x* axis in Figure 4, controls the leverage the regression method has in finding the best fit value of b. Prescribing std(log(*S*)) is useful because it may be possible to estimate probable values for *S* at a given field site before measuring it; mineral supply rates are often closely tied to denudation rates [e.g., *Heimsath et al*., 2012], which might be reflected in topography [*Granger et al*., 1996] or available in regional denudation rate measurements from other studies. This means that it may be possible to design studies at certain field sites with a priori estimates of *S*. Thus, prescribing std(log(*S*)) lets us explore how the spread in log(*S*) influences the method's statistical power, which may be useful in designing future field studies.

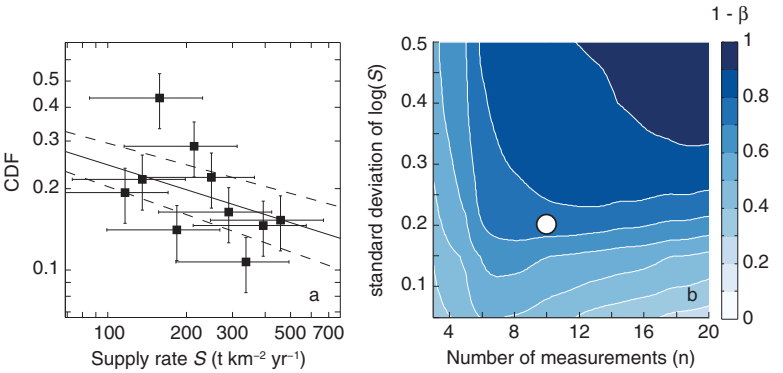

Figure 6. (a) An example of a synthetic data set generated in the Monte Carlo simulation that produced Figure 6b. (b) Statistical power of the test for supply-limited chemical erosion as a function of the number of data points, n, and the standard deviation of the log of supply rates, std(log(*S*)) (equation (5)). Darker colors indicate higher statistical power. White dot represents the example in Figure 6a. This shows that the test's reliability is highest at high values of both n and std(log(*S*)). Power values in this figure were smoothed with a rectangular window of width n = 2 and height log(std(*S*)) = 0.1.

We emphasize that the quantity of interest is the fractional spread in *S*—i.e., the spread in log(*S*)—and not the spread in *S* itself. This is because the regression parameters in equation (4) are determined from a regression of log(*CDF*) versus log(*S*) rather than a regression of *CDF* versus *S*. It is worth noting that because std(log(*S*)) is unrelated to std(*S*), the magnitude of the supply rates in any given data set is unimportant for these hypothesis tests.

In the Monte Carlo simulation, we constructed synthetic log(*CDF*) and log(*S*) data sets in three steps for each pair of n and std(log(*S*)) values. First, we generated values of log(*S*) by distributing n data points evenly in log(*S*), such that their standard deviation matched the prescribed std(log(*S*)). Second, for each synthetic data point, we generated a value of log(*CDF*) with the equation $\log(CDF) = a_s + b_s \log(S) + \varepsilon$, where ε is chosen at random from a normal distribution with mean = 0 and standard deviation = σ, and which represents the natural scatter around the trend. For this simulation, we used $a_s = 0$, $b_s = -0.3$, and $\sigma = 0.2$, values that lie within the ranges of the data sets in Table 1. Last, for each synthetic data point, we assigned uncertainties of 0.05 in log(*CDF*) and 0.1 in log(*S*), values similar to measurement uncertainties in the data sets in Table 1 (see supporting information Table S1). One representative synthetic data set generated in this way is shown in Figure 6a.

After generating each synthetic data set, we used Gaussian process regression to calculate best fit regression parameters $a \pm s_a$ and $b \pm s_b$ for $\log(CDF) = a + b \log(S)$. We then tested the null hypothesis of supply-limited chemical erosion ($b_0 = 0$) by comparing the t-value for the synthetic data set ($t = |b - b_0|/s_b$) to the critical t-value, $t_{\alpha,\nu}$, for a statistical significance $\alpha = 0.05$

We then tested the same null hypothesis by generating synthetic log(*CDF*) versus log(*S*) data sets at other pairs of n and std(log(*S*)) values. We did this over a range of n (from 3 to 20) and a range of std(log(*S*)) (from 0.05 to 0.5), which encompass the range of n and std(log(*S*)) values in the studies in Table 1.

For the final step in this Monte Carlo simulation, we generated 1000 synthetic data sets for each pair of n and std(log(*S*)) values, and tested the null hypothesis $b_0 = 0$ for each synthetic data set. The fraction of times the method correctly rejected the null hypothesis is an estimate of the method's statistical power ($1 - \beta$) at that pair of n and std(log(*S*)) values. In other words, it is the reliability of the test. Figure 6b shows the results of this Monte Carlo simulation: Statistical power is highest at high values of n and large spreads in log(*S*). Statistical power increases with increasing std(log(*S*)) because s_b decreases with std(log(*S*)). It increases with n because both s_b and $t_{\alpha,\nu}$ decrease with n (equation (5)). In the next section, we describe how Figure 6 can be used to guide future studies to maximize the chances of successfully testing hypotheses about supply-limited and kinetic-limited chemical erosion.

5.3. Improving Tests of Hypotheses About Limits to Chemical Erosion

The statistical power estimates in Figure 6b depend on the parameter values used in this Monte Carlo simulation—most importantly $|b - b_0| = 0.3$, $\sigma = 0.2$, and the uncertainties of 0.05 in log(*CDF*) and 0.1 in log(*S*))

on each synthetic data point. If $|b - b_0|$ were larger, for instance, the power would be higher, and if the scatter in log(*CDF*) around the trend were larger, the power would be lower. Nonetheless, the pattern of statistical power in Figure 6b is qualitatively similar to the pattern that would be seen for any parameter values used to estimate statistical power under the same Monte Carlo approach. It illustrates the basic point that statistical power should be highest at high values of n and std(log(*S*)) and lowest at low values of n and std(log(*S*)), regardless of the values of b, σ, and the measurement uncertainties.

The most valuable aspect of Figure 6b is that it quantifies the sensitivity of statistical power to the spread in log(*S*) and to n. Under the parameter values used in this simulation, Figure 6b suggests that to obtain a statistical power of at least 0.8 (a commonly chosen threshold), a data set must have a std(log(*S*))—i.e., a spread in the base 10 logarithm of supply rates—of at least 0.23. For a mean supply rate of 300 t km^2 yr^{-1}, the 95% confidence interval on the supply rates would need to be ~130–680 t km^2 yr^{-1}, spanning a range of roughly a factor of 5. Moreover, Figure 6b suggests that data sets with $n \leq 5$ will have low statistical power at any value of std(log(*S*)) < 0.5, a range that encompasses the range of std(log(*S*)) values in the compiled data sets (Table 1). For instance, only 8 of 16 studies in Figure 5 have a statistical power > 0.8 for a statistical significance $\alpha = 0.05$ under the null hypothesis that chemical erosion is supply limited ($b_0 = 0$).

5.4. Additional Factors That Can Affect b

The studies considered here were all conducted in granitic or schistose lithologies, mainly because measurements of denudation rates, interpreted here as a proxy for mineral supply rates, can be measured from cosmogenic nuclide concentrations in quartz. This does not mean, however, that chemical erosion rates are only limited by supply rates and kinetics in quartz-rich lithologies. The same limits should apply in any lithology. One asset of the statistical test presented here is that it can be applied to other lithologies with different dissolution kinetics than those in the studies considered here. Our results suggest that the chemical erosion rates in these regolith-based studies are more strongly influenced by supply rates than by dissolution kinetics. However, future measurements of *CDF* and mineral supply rates in other lithologies may display different relationships and may have different implications for tectonic feedbacks on Earth's long-term climate.

Other lithologies may display different sensitivities to supply and kinetics in part because they contain different mineral phases at different abundances. This could be elucidated by applying the same supply-limited and kinetic-limited framework to individual mineral phases, given sufficient data on mineral abundances in regolith and its parent rock. At present, few studies include colocated measurements of mineral abundances and supply rates [e.g., *Ferrier et al*., 2010], which hinders the application of this approach to individual mineral phases. This highlights the need for further studies with colocated measurements of supply rates and mineral abundances. Once such data are acquired, the relative influences of supply and kinetics could be interpreted in the context of the Damköhler number $D = k_i A_i Z/S$, which is the ratio between the regolith residence time, Z/S, and the characteristic timescale of mineral dissolution for phase i, $(k_i A_i)^{-1}$ [e.g., *Hilley et al*., 2010; *Lebedeva et al*., 2010; *Maher*, 2010]. Kinetic rate constants span several orders of magnitude across mineral phases, which implies that chemical erosion of some phases may be supply dominated while others are kinetic dominated, even in the same regolith. Such differences between phases could help explain the observed variation in b values among different studies. More generally, they could help explain the effects of supply and kinetics on chemical erosion in the bulk regolith in terms of their effects on individual mineral phases.

A related issue is that the parent lithology can set an effective upper limit on the bulk *CDF* for a given erosion rate and regolith thickness. For instance, a rock composed of 75% soluble phases (e.g., plagioclase, biotite, and hornblende) and 25% effectively insoluble phases over the regolith residence time (e.g., quartz) should have an effective upper limit of $CDF = 0.75$, except in places with extremely long regolith residence times. A potentially fruitful issue to explore in future studies is how chemically altered the regolith is relative to how altered it could possibly be, and to relate this to factors like supply, kinetics, and climate.

Mineral-specific analyses could also help reveal the relative contributions of silicates and carbonates to chemical erosion, a topic of longstanding interest due to the differing effects of carbonate and silicate weathering on the geologic carbon cycle [e.g., *Berner et al*., 1983; *West et al*., 2002]. Carbonate mineral phases like calcite are ubiquitous in granites and are highly soluble, but their concentrations in granites are so small that they do not significantly affect the *CDF*. Calcite, for instance, is typically found at

concentrations of ~0.1% in granites [*White et al*., 1999], and so can only affect the *CDF* by at most ~0.001. In applications to other lithologies with high carbonate concentrations, however, it is necessary to account for the carbonate-derived contribution to the *CDF* by other means if the goal is to extract the silicate-derived contribution.

Another factor that can affect *CDF* and thus the power law exponent in equation (4) is chemical erosion during downslope regolith transport, which can increase *CDF* with distance from the ridge [*Green et al*., 2006; *Mudd and Furbish*, 2006; *Yoo et al*., 2007]. For point measurements of supply rates (e.g., from soil production studies), the appropriate place to collect regolith for an analysis of *CDF* is at the ridge. Conversely, for catchment-wide estimates of supply rates (from cosmogenic nuclides in stream sediment), the appropriate place to collect regolith for *CDF*s is at the base of catchment slopes just before the material enters the channel. Not all the data from studies considered here came from the same geomorphic position on slopes. We have not attempted to assess the extent to which *CDF* values in these studies were influenced by differences in hillslope position, since the original studies did not assess that themselves. However, we note that variations in *CDF* due to downslope transport should only affect estimates of b to the extent that the influence of hillslope position on *CDF* covaries systematically with supply rates.

Another factor that could confound our proposed hypothesis tests on the power law slope b is a covariation of kinetics and supply rates, which could occur where supply rates covary with precipitation rates [e.g., *Reiners et al*., 2003; *Moon et al*., 2011; *Ferrier et al*., 2013]. This would tend to enhance dissolution at high supply rates [e.g., *Maher and Chamberlain*, 2014] and could lead to a more uniform pattern in *CDF* versus *S* than would be expected if climate were uniform across the sites. However, the potentially confounding effects of this complication on the power law slopes in Figure 5 are likely to be minimal, because precipitation and temperature do not vary substantially across the sites in most of the studies (Table 1). Nevertheless, it is worth pointing out that in larger, cross-site comparisons (including perhaps the "All sites" slope in Figure 5), covariations in climate and supply rates could theoretically cause a region with kinetically limited chemical erosion to appear to be supply limited. This would require unlikely scenarios in which, for example, supply rates increase with orographic precipitation rates and precipitation rates modulate chemical erosion rates in precisely the right proportions to transform the power law slope from $b = -1$ to $b = 0$. The extent to which this effect influences b values in studies that span a wide range of climates is a subject worthy of further research.

6. Conclusions

The central contributions of this study are a conceptual framework and a statistical test for supply-limited and kinetic-limited chemical erosion. Given the available types of field measurements, and the potential for spurious correlations, we recommend applying this test to regolith-based measurements of chemical depletion and mineral supply rates. These data types are determined independently, so goodness of fit values found in regressions that employ them will not be subject to spurious correlation.

Our analysis of published data sets suggests that the null hypothesis of supply-limited chemical erosion cannot be rejected for 8 of 16 cases. Meanwhile, the null hypothesis of kinetic-limited chemical erosion cannot be rejected for just one of the cases. For the remaining cases, mean values of b lie between 0 and −0.5. To the extent that values of b reflect the relative importance of supply and kinetics and driving chemical erosion, this suggests that chemical erosion is influenced by both supply rates and dissolution kinetics, but more strongly by supply rates. This conclusion, which is derived solely from measurements in regolith, provides a point of comparison to measurements of fluvial fluxes, which suggest that chemical erosion in some basins may be far from supply limited [e.g., *Viers et al*., 2009; *Lupker et al*., 2012].

We conducted a statistical power analysis to illustrate the method's reliability as a function of the number of measurements and the variability in supply rates in the measured data. Such analyses can help guide design of studies that wish to test hypotheses about supply-limited and kinetic-limited chemical erosion across other sites. Our analyses suggest that most of the field studies considered here have high uncertainties and thus low statistical power, either because they contain few measurements—13 of the 15 studies have fewer than 8 measurements—or because they span a narrow range in mineral supply rates. This is not a criticism of previous work; many of the measurements were designed to answer questions not related to supply-limited and kinetic-limited chemical erosion. Moreover, measuring rates of mineral supply and

chemical erosion can be costly and labor intensive. Nevertheless, we suggest that future studies of supply-limited and kinetic-limited chemical erosion will be best served by designing studies with more measurements across a wider range of mineral supply rates, while minimizing the effects of potentially confounding factors such as differences in climate and lithology.

Acknowledgments
We thank Jim Kirchner, Bob Kopp, and Dario Grana for helpful discussions. We thank George Hilley, one anonymous reviewer, and editor Cin-Ty Lee for comments that substantially improved this manuscript. The data used are listed in the references, tables, and supporting information. This work was supported in part by NSF EAR 1331939.

References

Anderson, R. S. (2015), Particle trajectories on hillslopes: Implications for particle age and ^{10}Be structure, *J. Geophys. Res. Earth Surf.*, *120*, 1626–1644, doi:10.1002/2015JF003479.

Anderson, S. P., W. E. Dietrich, and G. H. Brimhall (2002), Weathering profiles, mass-balance analysis, and rates of solute loss: Linkages between weathering and erosion in a small, steep catchment, *Geol. Soc. Am. Bull.*, *114*(9), 1143–1158.

Bensen, M. A. (1965), Spurious correlation in hydraulics and hydrology, *J. Hydraul. Div. Am. Soc. Civ. Eng.*, *91*, 3542.

Berner, R. A., A. C. Lasaga, and R. M. Garrels (1983), The carbonate-silicate geochemical cycle and its effect on atmospheric carbon-dioxide over the past 100 million years, *Am. J. Sci.*, *283*, 641–683.

Brantley, S. L., and M. Lebedeva (2011), Learning to read the chemistry of regolith to understand the Critical Zone, *Annu. Rev. Earth Planet. Sci.*, *39*, 387–416, doi:10.1146/annurev-earth-040809-152321.

Brantley, S. L., and A. F. White (2009), Approaches to modeling weathering regolith, *Rev. Mineral. Geochem.*, *70*, 435–484.

Brantley, S. L., M. E. Holleran, L. Jin, and E. Bazilevskaya (2013), Probing deep weathering in the Shale Hills Critical Zone Observatory, Pennsylvania (USA): The hypothesis of nested chemical reaction fronts in the subsurface, *Earth Surf. Processes Landforms*, *38*, 1280–1298.

Brett, M. T. (2004), When is a correlation between non-independent variables "spurious"?, *Oikos*, *105*, 647–656.

Brimhall, G. H., and W. E. Dietrich (1987), Constitutive mass balance relations between chemical composition, volume, density, porosity, and strain in metasomatic hydrochemical systems: Results on weathering and pedogenesis, *Geochim. Cosmochim. Acta*, *51*(3), 567–587.

Brimhall, G. H., C. J. Lewis, J. J. Ague, W. E. Dietrich, J. Hampel, T. Teague, and P. Rix (1988), Metal enrichment in bauxites by deposition of chemically mature aeolian dust, *Nature*, *333*, 819–824.

Brown, E. T., R. F. Stallard, M. C. Larsen, G. M. Raisbeck, and F. Yiou (1995), Denudation rates determined from the accumulation of in situ-produced ^{10}Be in the Luquillo Experimental Forest, Puerto Rico, *Earth Planet. Sci. Lett.*, *129*, 193–202.

Burke, B. C., A. M. Heimsath, J. L. Dixon, J. Chappell, and K. Yoo (2009), Weathering the escarpment: Chemical and physical rates and processes, south-eastern Australia, *Earth Surf. Processes Landforms*, *34*, 768–785, doi:10.1002/esp.1764.

Chayes, F. (1949), On ratio correlation in petrography, *J. Geol.*, *57*, 239–254.

Colbourn, G., A. Ridgwell, and T. M. Lenton (2015), The timescale of the silicate weathering negative feedback on atmospheric CO_2, *Global Biogeochem. Cycles*, *29*, 583–596, doi:10.1002/2014GB005054.

Dixon, J. L., A. M. Heimsath, and R. Amundson (2009a), The critical role of climate and saprolite weathering in landscape evolution, *Earth Surf. Processes Landforms*, *34*, 1507–1521, doi:10.1002/esp.1836.

Dixon, J. L., A. M. Heimsath, J. Kaste, and R. Amundson (2009b), Climate-driven processes of hillslope weathering, *Geology*, *37*, 975–978, doi:10.1130/G30045A.1.

Dixon, J. L., A. S. Hartshorn, A. M. Heimsath, R. A. DiBiase, and K. X. Whipple (2012), Chemical weathering response to tectonic forcing. A soils perspective from the San Gabriel Mountains, California, *Earth Planet. Sci. Lett.*, *323*, 40–49.

Dosseto, A., H. L. Buss, and P. O. Suresh (2012), Rapid regolith formation over volcanic bedrock and implications for landscape evolution, *Earth Planet. Sci. Lett.*, *337–338*, 47–55.

Drever, J. I. (1994), The effect of land plants on weathering rates of silicate minerals, *Geochem. Cosmochim. Acta*, *58*, 2325–2332.

Ferrier, K. L., and J. W. Kirchner (2008), Effects of physical erosion on chemical denudation rates: A numerical modeling study of soil-mantled hillslopes, *Earth Planet. Sci. Lett.*, *272*, 591–599.

Ferrier, K. L., J. W. Kirchner, C. S. Riebe, and R. C. Finkel (2010), Mineral-specific chemical weathering rates over millennial timescales: Measurements at Rio Icacos, *Puerto Rico, Chem. Geol.*, *277*, 101–114.

Ferrier, K. L., J. W. Kirchner, and R. C. Finkel (2011), Estimating millennial-scale rates of dust incorporation into eroding hillslope soils using cosmogenic nuclides and immobile weathering tracers, *J. Geophys. Res.*, *116*, F03022, doi:10.1029/2011JF001991.

Ferrier, K. L., J. W. Kirchner, and R. C. Finkel (2012), Weak influences of climate and physical erosion rates on chemical erosion rates: Measurements along two altitudinal transects in the Idaho Batholith, *J. Geophys. Res.*, *117*, F02026, doi:10.1029/2011JF002231.

Ferrier, K. L., J. T. Perron, S. Mukhopadhyay, M. Rosener, J. D. Stock, K. L. Huppert, and M. Slosberg (2013), Covariation of climate and long-term erosion rates across a steep rainfall gradient on the Hawaiian island of Kaua'i, *Geol. Soc. Am. Bull.*, *125*, 1146–1163, doi:10.1130/B30726.1.

Foster, M. A., R. S. Anderson, C. E. Wyshnytzky, W. B. Ouimet, and D. P. Dethier (2015), Hillslope lowering rates and mobile-regolith residence times from in situ and meteoric ^{10}Be analysis, Boulder Creek Critical Zone Observatory, Colorado, *Geol. Soc. Am. Bull.*, *127*, 862, doi:10.1130/B31115.1.

Gabet, E. J., and S. M. Mudd (2009), A theoretical model coupling chemical weathering rates with denudation rates, *Geology*, *37*, 151–154.

Galat, D. L. (1990), Estimating fluvial mass transport to lakes and reservoirs: Avoiding spurious self-correlation, *Lake Reservoir Manage.*, *6*, 153–163.

Garrels, R. M., and F. T. Mackenzie (1967), Origin of the chemical composition of some springs and lakes, in *Equilibrium Concepts in Natural Water Systems*, Am. Chem. Soc., Washington, D. C.

Godsey, S., J. Kirchner, and D. Clow (2009), Concentration-discharge relationships reflect chemostatic characteristics of US catchments, *Hydrol. Processes*, 1864, 1844−1864.

Granger, D. E., J. W. Kirchner, and R. Finkel (1996), Spatially averaged long-term erosion rates measured from in situ-produced cosmogenic nuclides in alluvial sediment, *J. Geol.*, *104*, 249–257.

Green, E. G., W. E. Dietrich, and J. F. Banfield (2006), Quantification of chemical weathering rates across an actively eroding hillslope, *Earth Planet. Sci. Lett.*, *242*, 155–169.

Hay, C. C., E. Morrow, R. E. Kopp, and J. X. Mitrovica (2015), Probabilistic reanalysis of twentieth-century sea-level rise, *Nature*, *517*, 481–484, doi:10.1038/nature14093.

Heimsath, A. M., W. E. Dietrich, K. Nishiizumi, and R. C. Finkel (1997), The soil production function and landscape equilibrium, *Nature*, *388*, 358–361.

Heimsath, A. M., R. A. DiBiase, and K. X. Whipple (2012), Soil production limits and the transition to bedrock dominated landscapes, *Nat. Geosci.*, *5*, 210–214.

Hilley, G. E., C. P. Chamberlain, S. Moon, S. Porder, and S. D. Willett (2010), Competition between erosion and reaction kinetics in controlling silicate-weathering rates, *Earth Planet. Sci. Lett.*, *293*, 191–199.
Jin, L., R. Ravella, B. Ketchum, P. R. Bierman, P. Heaney, T. White, and S. L. Brantley (2010), Mineral weathering and elemental transport during hillslope evolution at the Susquehanna/Shale Hills Critical Zone Observatory, *Geochim. Cosmochim. Acta*, *74*, 3669–3691.
Kenney, B. C. (1982), Beware of spurious self-correlation!, *Water Resour. Res.*, *18*, 1041–1048.
Kirchner, J. W., and K. L. Ferrier (2013), Mainly in the plain, *Nature*, *495*, 318–319.
Kirchner, J. W., R. C. Finkel, C. S. Riebe, D. E. Granger, J. L. Clayton, J. G. King, and W. F. Megahan (2001), Mountain erosion over 10 yr, 10 k.y., and 10 m.y. time scales, *Geology*, *29*, 591–594.
Larsen, I. J., P. C. Almond, A. Eger, J. O. Stone, D. R. Montgomery, and B. Malcolm (2014a), Rapid soil production and weathering in the Southern Alps, New Zealand, *Science*, *343*, 637–640.
Larsen, I. J., D. R. Montgomery, and H. M. Greenberg (2014b), The contribution of mountains to global denudation, *Geology*, *42*, 527–530.
Lebedeva, M. I., R. C. Fletcher, and S. L. Brantley (2010), A mathematical model for steady-state regolith production at constant erosion rate, *Earth Surf. Processes Landforms*, *35*, 508–524.
Lee, C. A., S. Thurner, S. Paterson, and W. Cao (2015), The rise and fall of continental arcs: Interplays between magmatism, uplift, weathering, and climate, *Earth Planet. Sci. Lett.*, *425*, 105–119.
Likens, G. E., F. H. Bormann, N. M. Johnson, and R. S. Pierce (1967), The calcium, magnesium, potassium, and sodium budgets for a small forested ecosystem, *Ecology*, *48*, 772–785.
Lucas, Y. (2001), The role of plants in controlling rates and products of weathering: Importance of biological pumping, *Annu. Rev. Earth Planet. Sci.*, *29*, 135–163.
Lukens, C. E., C. S. Riebe, L. S. Sklar, and D. L. Shuster (2016), Grain size bias in cosmogenic nuclide studies of stream sediment in steep terrain, *J. Geophys. Res.*, doi:10.1002/2016JF003859.
Lupker, M., C. France-Lanord, V. Galy, J. Lavé, J. Gaillardet, A. P. Gajurel, and R. Sinha (2012), Predominant floodplain over mountain weathering of Himalayan sediments (Ganga basin), *Geochim. Cosmochim. Acta*, *84*, 410–432.
Maher, K. (2010), The dependence of chemical weathering rates on fluid residence time, *Earth Planet. Sci. Lett.*, *294*, 101–110.
Maher, K., and C. P. Chamberlain (2014), Hydrologic regulation of chemical weathering and the geologic carbon cycle, *Science*, *343*, 1502–1504, doi:10.1126/science.1250770.
Marchand, D. E. (1970), Soil contamination in the White Mountains, eastern California, *Geol. Soc. Am. Bull.*, *81*, 2497–2506.
Marshall, C. E., and J. F. Haseman (1942), The quantitative evolution of soil formation and development by heavy mineral studies: A Grundy silt loam profile, *Soil Sci. Soc. Am. J.*, *7*, 448–453.
Merrill, G. P. (1897), *A Treatise on Rocks, Rock-Weathering and Soils*, 411 pp., Macmillan, N. Y.
Moon, S., C. P. Chamberlain, K. Blisniuk, N. Levine, D. H. Rood, and G. E. Hilley (2011), Climatic control of denudation in the deglaciated landscape of the Washington Cascades, *Nat. Geosci.*, *4*, 469–473, doi:10.1038/ngeo1159.
Mudd, S. M., and D. J. Furbish (2006), Using chemical tracers in hillslope soils to estimate the importance of chemical denudation under conditions of downslope sediment transport, *J. Geophys. Res.*, *111*, F02021, doi:10.1029/2005JF000343.
Niemi, N. A., M. Oskin, D. W. Burbank, A. M. Heimsath, and E. J. Gabet (2005), Effects of bedrock landslides on cosmogenically determined erosion rates, *Earth Planet. Sci. Lett.*, *237*, 480–498.
Norton, K. P., and F. von Blanckenburg (2010), Silicate weathering of soil-mantled slopes in an active alpine landscape, *Geochim. Cosmochim. Acta*, *74*, 5243–5258.
Pearson, K. (1897), On a form of spurious correlation which may arise when indices are used in the measurement of organs, *Proc. R. Soc. London*, *60*, 489–502.
Rasmussen, C., S. Brantley, D. deB. Richter, A. Blum, J. Dixon, and A. F. White (2011), Strong climate and tectonic control on plagioclase weathering in granitic terrain, *Earth Planet. Sci. Lett.*, *301*, 521–530.
Rasmussen, C. E., and C. K. L. Williams (2006), *Gaussian Processes for Machine Learning*, MIT Press, Massachusetts Institute of Technology.
Raymo, M. E., W. F. Ruddiman, and P. N. Froelich (1988), Influence of late Cenozoic mountain building on ocean geochemical cycles, *Geology*, *16*, 649–653.
Reed, J. L. (1921), On the correlation between any two functions and its application to the general case of spurious correlation, *J. Wash. Acad. Sci.*, *11*, 449–455.
Reiners, P. W., T. A. Ehlers, S. G. Mitchell, and D. R. Montgomery (2003), Coupled spatial variations in precipitation and long-term erosion rates across the Washington Cascades, *Nature*, *426*, 645–647.
Rex, R. W., J. K. Syers, M. L. Jackson, and R. N. Clayton (1969), Eolian origin of quartz in soils of the Hawaiian islands and in Pacific pelagic sediments, *Science*, *163*, 277–279.
Riebe, C. S., J. W. Kirchner, D. E. Granger, and R. C. Finkel (2001), Strong tectonic and weak climatic control of long-term chemical weathering rates, *Geology*, *29*, 511–514.
Riebe, C. S., J. W. Kirchner, and R. C. Finkel (2003), Long-term rates of chemical weathering and physical erosion from cosmogenic nuclides and geochemical mass balance, *Geochim. Cosmochim. Acta*, *67*, 4411–4427.
Riebe, C. S., J. W. Kirchner, and R. C. Finkel (2004a), Sharp decrease in long-term chemical weathering rates along an altitudinal transect, *Earth Planet. Sci. Lett.*, *218*, 421–434.
Riebe, C. S., J. W. Kirchner, and R. C. Finkel (2004b), Erosional and climatic effects on long-term chemical weathering rates in granitic landscapes spanning diverse climate regimes, *Earth Planet. Sci. Lett.*, *224*, 547–562.
Riebe, C. S., L. S. Sklar, C. E. Lukens, and D. L. Shuster (2015), Climate and topography control the size and flux of sediment produced on steep mountain slopes, *Proc. Natl. Acad. Sci. U. S. A.*, *112*, 15,574–15,579.
Stallard, R. (1985), River chemistry, geology, geomorphology, and soils in the Amazon and Orinoco Basins, in *The Chemistry of Weathering, NATO ASI Ser.*, vol. 149, edited by J. Drever, pp. 293–316, Springer, Dordrecht, Netherlands.
Stallard, R. F., and J. M. Edmond (1983), Geochemistry of the Amazon 2. The influence of geology and weathering environment on the dissolved load, *J. Geophys. Res.*, *88*, 9671–9688.
Torres, M., A. J. West, and K. E. Clark (2015), Geomorphic regime modulates hydrologic control of chemical weathering in the Andes-Amazon, *Geochim. Cosmochim. Acta*, *166*, 105–128.
Viers, J., B. Dupré, and J. Gaillardet (2009), Chemical composition of suspended sediments in World Rivers: New insights from a new database, *Sci. Total Environ.*, *407*, 853–868.
Waldbauer, J. R., and C. P. Chamberlain (2005), Influence of uplift, weathering and base cation supply on past and future CO_2 levels, in *A History of Atmospheric CO_2 and Its Effects on Plants, Animals, and Ecosystems. Ecological Studies*, vol. 177, edited by J. R. Ehleringer, T. E. Cerling, and M. D. Dearing, pp. 166–184, Springer, N. Y.

Walker, J. C. G., P. B. Hays, and J. F. Kasting (1981), A negative feedback mechanism for the long-term stabilization of Earth's surface temperature, *J. Geophys. Res.*, *86*, 9776–9782.

West, A. J. (2012), Thickness of the chemical weathering zone and implications for erosional and climatic drivers of weathering and for carbon-cycle feedbacks, *Geology*, *40*, 811, doi:10.1130/G33041.1.

West, A. J., M. J. Bickle, R. Collins, and J. Brasington (2002), Small-catchment perspective on Himalayan weathering fluxes, *Geology*, *30*, 355–358.

West, A. J., A. Galy, and M. Bickle (2005), Tectonic and climatic controls on silicate weathering, *Earth Planet. Sci. Lett.*, *235*, 211–228.

West, A. J., R. Hetzel, G. Li, Z. Jin, F. Zhang, R. G. Hilton, and A. L. Densmore (2014), Dilution of ^{10}Be in detrital quartz by earthquake-induced landslides: Implications for determining denudation rates and potential to provide insights into landslide sediment dynamics, *Earth Planet. Sci. Lett.*, *396*, 143–153.

White, A. F., A. E. Blum, M. S. Schulz, D. V. Vivit, D. A. Stonestrom, M. Larsen, S. F. Murphy, and D. Eberl (1998), Chemical weathering in a tropical watershed, Luquillo Mountains, Puerto Rico: I. Long-term versus short-term weathering fluxes, *Geochim. Cosmochim. Acta*, *62*, 209–226.

White, A. F., T. D. Bullen, D. V. Vivit, M. S. Schulz, and D. W. Clow (1999), The role of disseminated calcite in the chemical weathering of granitoid rocks, *Geochim. Cosmochim. Acta*, *63*, 1939–1953.

Willenbring, J. K., A. T. Codilean, and B. McElroy (2013), Earth is (mostly) flat: Apportionment of the flux of continental sediment over millennial time scales, *Geology*, *41*, 343–346.

Yanites, B. J., G. E. Tucker, and R. S. Anderson (2009), Numerical and analytical models of cosmogenic radionuclide dynamics in landslide-dominated drainage basins, *J. Geophys. Res.*, *114*, F01007, doi:10.1029/2008JF001088.

Yoo, K., and S. M. Mudd (2008), Toward process-based modeling of geochemical soil formation across diverse landforms: A new mathematical framework, *Geoderma*, *146*, 248–260.

Yoo, K., R. Amundson, A. M. Heimsath, W. E. Dietrich, and G. H. Brimhall (2007), Integration of geochemical mass balance with sediment transport to calculate rates of soil chemical weathering and transport on hillslopes, *J. Geophys. Res.*, *112*, F02013, doi:10.1029/2005JF000402.

Zar, J. (1999), *Biostatistical Analysis*, 4th ed., 663 pp., Prentice Hall, N. J.